[CANCER RESEARCH 64, 9012–9017, December 15, 2004]

The Minimal Active Domain of Endostatin Is a Heparin-Binding Motif that Mediates Inhibition of Tumor Vascularization

Anna-Karin Olsson,[1] Irja Johansson,[1] Helena Åkerud,[1] Barbro Einarsson,[2] Rolf Christofferson,[2] Takako Sasaki,[3] Rupert Timpl,[3] and Lena Claesson-Welsh[1]

[1]Department of Genetics and Pathology, Uppsala University, Rudbeck Laboratory, Uppsala, Sweden; [2]Department of Medical Cell Biology, Biomedical Centre, Uppsala, Sweden; and [3]Laboratory of Protein Chemistry, Max-Planck Institute for Biochemistry, Martinsried, Germany

ABSTRACT

Endostatin constitutes the COOH-terminal 20,000 Da proteolytic fragment of collagen XVIII and has been shown to possess antiangiogenic and antitumorigenic properties. In the present study, we have investigated the role of the heparin-binding sites in the *in vivo* mechanism of action of endostatin. The majority of the heparin binding is mediated by arginines 155/158/184/270 in endostatin, but there is also a minor site constituted by arginines 193/194. Using endostatin mutants lacking either of these two sites, we show that inhibition of fibroblast growth factor-2–induced angiogenesis in the chicken chorioallantoic membrane requires both heparin-binding sites. In contrast, inhibition of vascular endothelial growth factor-A–induced chorioallantoic membrane angiogenesis by endostatin was only dependent on the minor heparin-binding site (R193/194). These arginines were also required for endostatin to inhibit fibroblast growth factor-2– and vascular endothelial growth factor-A–induced chemotaxis of primary endothelial cells. Moreover, we show that a synthetic peptide corresponding to amino acids 180–199 of human endostatin (which covers the minor heparin-binding site) inhibits endothelial cell chemotaxis and reduces tumor vascularization *in vivo*. Substitution of arginine residues 193/194 for alanine attenuates the antiangiogenic effects of the peptide. These data show an essential role for heparin binding in the antiangiogenic action of endostatin.

INTRODUCTION

Angiogenesis, formation of new capillary blood vessels, is essential during development and in physiologic conditions such as wound healing and the menstrual cycle (1). However, prolonged and excessive angiogenesis has been implicated in different pathologic processes, *e.g.*, tumor growth (2–5). Blood vessel formation in the body is tightly regulated by a number of positive and negative factors. The tyrosine kinase receptor ligands, fibroblast growth factor (FGF) and vascular endothelial growth factor (VEGF), are examples of extensively studied stimulators of angiogenesis (6–8). The positive signals for blood vessel formation are counteracted by antiangiogenic molecules, among which endostatin (9) is one of the best characterized (see ref. 10 for review).

Endostatin constitutes the COOH-terminal 20,000 Da proteolytic fragment of collagen XVIII (9). Treatment with endostatin has been shown to inhibit or reduce tumor growth in several experimental animal models (10). Endostatin is present in plasma (10), platelets (11) and the basement membrane of blood vessels (12), where it can bind extracellular matrix proteins such as fibulin-1 and -2 (13). In a recent study by Yu *et al.* (14), the leukocyte adhesion antigen E-selectin was shown to be required for the antiangiogenic effect of endostatin *in vivo* and to confer endostatin sensitivity to nonresponsive endothelial cells *in vitro*. Endostatin has also been shown to interact with heparin/heparan sulfate (15) linked, *e.g.*, to the heparan sulfate proteoglycans glypican-1 and -4 (16) and with $\alpha5\beta1$ integrins (17). Several studies show that $\alpha5\beta1$ is an important mediator of the antiangiogenic effect of endostatin (18–20). A critical role for heparin/heparan sulfates in endostatin-induced inhibition of angiogenesis has also been reported previously (15, 21), and heparan sulfate proteoglycans have been shown to mediate the downstream intracellular signaling events induced by endostatin (19, 21). However, there is one report stating that VEGF-induced chemotaxis of endothelial cells, a commonly used surrogate assay for angiogenesis, is inhibited by mutated endostatin lacking heparin-binding ability (22). These apparent discrepancies with respect to the significance of heparin/heparan sulfates for the angiogenic response may be attributable to the use of different angiogenic stimuli (FGF *versus* VEGF) or the choice of angiogenesis assay.

In this study we have further investigated the role of the heparin/heparan sulfate-binding motifs in endostatin for its antiangiogenic function, both *in vitro* and *in vivo*. Two heparin-binding sites have been identified in endostatin; a major (arginines 155/158/184/270) and a minor (arginines 193/194; ref. 15, 23). The heparin binding to endostatin is mediated via a unique sequence in the heparin/heparan sulfate chain (24). By using mutated forms of endostatin, lacking either of the heparin-binding sites, we show that only the minor heparin-binding site (R193/194A) is critical for the ability of endostatin to inhibit both FGF-2– and VEGF-A–induced angiogenesis in the chicken chorioallantoic membrane (CAM). Administration of a synthetic peptide corresponding to a stretch covering amino acid residues R193/194 [peptide 180–199/wild-type (wt)], but not of a mutated R193/194A peptide [peptide 180–199/mutant (mut)], led to reduced vascularization of mouse fibrosarcoma in C57BL6/J mice. Vascularization of human pancreatic tumors in nude mice was also reduced after treatment with peptide 180–199/wt, compared with treatment with peptide 180–199/mut. Thus, these studies define the minimal active domain of endostatin in its antiangiogenic action.

MATERIALS AND METHODS

Endostatin Mutants and Synthetic Peptides. Wild-type endostatin as well as the mutants R158/184/270A and R193/194A were produced by expression in human embryonic kidney 293-Epstein-Barr virus nuclear antigen cells, as described previously (13). Briefly, a mouse endostatin vector was used that also served as a template to introduce single to triple point mutations by appropriate pairs of overlapping oligonucleotides and fusion PCR (25, 26). Recombinant protein was purified by heparin-Sepharose and Superose 12 chromatography, from serum-free culture medium conditioned by transfected 293-Epstein-Barr virus nuclear antigen cells. A full description of the proteins is given in (15). Recombinant human endostatin (EntreMed Inc.) produced in *Pichia pastoris* was used in the animal studies. All endostatin preparations were tested for endotoxin activity and were found to be essentially free of contamination.

Peptide 180–199/wt is a synthetic peptide corresponding to amino acids 180–199 of human endostatin and has the following sequence: FLSSRLQDLYSIVRRADRAA-COOH. A peptide where arginine residues 193 and 194

Received 6/21/04; revised 8/23/04; accepted 9/17/04.

Grant support: from the Swedish Cancer Society (project no 3820-B01–06XAC; grant to L. Claesson-Welsh).

The costs of publication of this article were defrayed in part by the payment of page charges. This article must therefore be hereby marked *advertisement* in accordance with 18 U.S.C. Section 1734 solely to indicate this fact.

Note: I. Johansson and H. Åkerud contributed equally to the work. R. Timpl is deceased.

Requests for reprints: Anna-Karin Olsson, Department of Genetics and Pathology, Uppsala University, Dag Hammarskjöldväg20, Uppsala, 751 85, Sweden. Phone: 46-18-471-46-07; Fax: 011-46-18-55-89-31; E-mail: Anna-Karin.Olsson@genpat.uu.se.

were substituted for alanine was also synthesized (peptide 180–199/mut). The peptides were purchased from AnaSpec Inc. Amino acid residue numbers refer to the entire noncollagenous domain of 315 amino acid residues, where endostatin constitutes residues 132–315.

Cell Culture. Primary bovine adrenal cortex capillary endothelial (BCE) cells were cultured on gelatin- coated dishes in DMEM/10% newborn calf serum, 2 ng/mL FGF-2 (PeproTech, Inc., Rocky Hill, NJ). Media and serum were from Life Technologies, Inc. (Rockville, MD). For chemotaxis assays, BCE cells were serum-starved over night in 0.5% newborn calf serum.

Chorioallantoic Membrane Assay. The conditions for the chorioallantoic membrane (CAM) assay were as described previously (21, 27). FGF-2 (Boehringer Mannheim, Ingelheim, Germany) and VEGF-A (PeproTech, Inc.) were used at 0.2 μg/filter, endostatin was used at 0.3, 3, or 15 μg/filter, and endostatin mutants were used at 3 or 15 μg/filter. Ten-day-old embryos were used, and the treatment period was 3 days. The treated CAMs were inspected in a light microscope, and the score, from 1 (low) to 4 (high) was based on the number of vessel branch points. Average values for five to eight embryos per treatment were recorded.

Chemotaxis Assay. Chemotaxis assays were performed using a modified Boyden chamber as described previously (28), with 8-μm micropore polycarbonate filters (PFB8–50, Neuro Probe Inc., Gaithersburg, MD) coated with type-1 collagen solution at 100 μg/mL (Vitrogen 100, Collagen Corp., Palo Alto CA). BCE cells that had been starved over night in 0.5% newborn calf serum were trypsinized and resuspended at 7.5×10^5 cells/mL in DMEM, 0.25% BSA, and Trasylol at 1,000 kallikrein-inactivating units (KIU). The cell suspension was added in the upper chamber and growth factors, FGF-2 (10 ng/mL; PeproTech, Inc.) or VEGF-A (10 ng/mL, PeproTech, Inc.), in the lower chamber. Endostatin, endostatin mutants, and synthetic peptides were added both in the upper and in the lower chamber at indicated concentrations. After 5 hours at 37°C, we stained cells that had migrated through the filter with Giemsa and counted them using the "Easy Image Analysis" software (Tekno Optik AB, Skärholmen, Sweden). All samples were analyzed in at least six wells for each treatment and at several separate occasions. We calculated the significance at the level of $P < 0.05$ using Student's t test.

Animal Studies. Animal work was approved by the Uppsala University board of animal experimentation and thus done according to the UKCCCR guidelines for the welfare of animals in experimental neoplasia (29). The mice were anesthetized with isoflurane (Forene, Abbott Laboratories, Abbott Park, IL) during all manipulations.

For the fibrosarcoma study, 5-week-old female C57BL6/J mice (Møllegaard-Bomholtgaard, Ry, Denmark) were injected with 0.5×10^6 T241 fibrosarcoma cells subcutaneously into the left flank. Animals carrying palpable tumors (approximately 50 mm^3) were randomized (n = 5–6 animals/treatment group) and received treatment with endostatin or either of the two synthetic peptides (180–199/wt and 180–199/mut), all at 25 mg/kg/day. Human IgG was used as control. The treatments were given as daily subcutaneous injections in the right flank for 11 days. The tumors were measured with a caliper once a day, in a blind procedure, and volumes were calculated by the formula $\pi/6 \times \text{width}^2 \times$ length.

For the pancreatic carcinoma study, 6-week-old female Fox Chase SCID mice were injected subcutaneously with 2.5×10^6 BxPC3 pancreatic carcinoma cells. When tumors had reached a size of approximately 100 mm^3, the animals were randomized (n = 10 animals/treatment group) and treatment with 180–199/wt and 180–199/mut, at 25 mg/kg/day, was initiated. We delivered the peptides using mini-osmotic pumps implanted intraperitoneally. The type of pump used in these experiments (1007D, ALZET, Cupertino, CA), distributes 0.5 μL/hour for 7 days. The length of the treatment period at the specified dose required a change of the osmotic pump after one week of treatment, *i.e.*, in total three surgical procedures on each mouse in the study. The tumors were measured with a caliper, in a blind procedure, and volumes were calculated by the formula $\pi/6 \times \text{width}^2 \times$ length. One animal in each treatment group was euthanized during the study because of peritoneal infection. At least three animals in each treatment group from both the T241 and the BxPC3 study were perfused with 4% paraformaldehyde in PBS (pH 7.4; T241) or 4% paraformaldehyde in 300 mOsm Millonigbuffer (pH 7.4; BxPC3). Tumors were embedded in paraffin according to standard histologic procedures and sectioned at 3 μm.

CD31 Staining and Quantification of Vascular Parameters. Paraffin sections of T241 fibrosarcoma tumors were stained immunohistochemically using a goat antimouse CD31 antibody (1506, Santa Cruz Biotechnology, Santa Cruz, CA), diluted 1:500, and incubated at 4°C over night. Detection of the primary antibody binding sites was done with a biotinylated antigoat antibody (BA-5000, Vector Laboratories, Burlingame, CA) and streptavidin-horseradish peroxidase (SA-5004, Vector Laboratories) with an amplification step (TSA Biotin System, Perkin-Elmer, Fremont, CA). We visualized the enzymatic signal using 3-amino-9-ethylcarbazole peroxidase substrate kit (SK-4200, Vector Laboratories). BxPC3 pancreatic carcinoma tumors were stained using the same CD31 antibody as above but diluted 1:50 and incubated at 4°C over night. Detection of the primary antibody binding sites was done with the same biotinylated antigoat antibody as above, together with avidin-biotin complex method complex/horseradish peroxidase kit (K0355, Dako). We visualized immunoreactivity using 3-amino-9-ethylcarbazole peroxidase substrate kit (above). Stereological quantification of vascular parameters was done as described previously (30). We calculated significance at the level of $P < 0.05/0.1$ using Student's t test.

RESULTS

Endostatin Inhibits FGF-2– and VEGF-A–Induced Angiogenesis in the Chicken Chorioallantoic Membrane via Distinct Heparin-Binding Motifs. Angiogenesis in the chicken CAM of 10-day-old chicken embryos was stimulated by application of FGF-2 and VEGF-A (Table 1). The extent of the angiogenic response was estimated by scoring on a scale from 1 to 4, according to Friedlander *et al.* (27). Endostatin (ES) efficiently inhibited FGF-2–induced CAM angiogenesis at a 10-fold molar excess (3 μg) but had no effect on VEGF-A–induced angiogenesis at this dose. When increasing the endostatin dose to 15 μg/CAM, the VEGF-A–induced angiogenic response was decreased although not completely suppressed. To examine the role of the heparin-binding ability of ES for the antiangiogenic effect, we analyzed the characteristics of two endostatin mutants using the CAM assay. The mutant R158/184/270A lacks the major heparin-binding site, which confers most of the heparin-binding ability. The other mutant, R193/194A, lacks the minor heparin-binding site. When tested on FGF-2–stimulated CAM angiogenesis, the R158/184/270A mutant showed loss-of-function characteristics and failed to inhibit the angiogenic response when added at 3 μg/CAM. However, the R158/184/270A mutant still inhibited VEGF-A–stimulated angiogenesis with similar efficiency as wild-type ES, when added at 15 μg/CAM. In contrast, the R193/194 heparin-binding mutant failed to inhibit both FGF-2– and VEGF-A–induced angiogenesis. These results indicate that the heparin-binding ability of endostatin conferred by the minor heparin-binding site (R193/194) is critical for its antiangiogenic effect in the CAM.

Effect of the R193/194A Endostatin Mutant on Endothelial Cell Chemotaxis. To further investigate the role of the arginine residues at position 193/194 in endostatin for its inhibitory effect on FGF-2– and VEGF-A–stimulated endothelial cells, we did chemotaxis assays using primary BCE cells. FGF-2 induced a close to 2-fold increase in

Table 1 *Inhibitory effect of endostatin and endostatin heparin-binding mutants on chicken CAM angiogenesis induced by FGF-2 or VEGF-A*

Stimulator	Inhibitor	Angiogenesis score (mean)	No. of embryos
Buffer	None	1.1	8
FGF-2, 0.2 μg	None	3.2	8
	ES, 0.3 μg	3.0	5
	ES, 3 μg	1.1	8
VEGF-A, 0.2 μg	None	3.3	8
	ES, 3 μg	3.2	5
	ES, 15 μg	2.0	7
FGF-2, 0.2 μg	R158/184/270A, 3 μg	2.8	7
	R158/184/270A, 15 μg	3.0	5
	R193/194A, 3 μg	2.9	7
VEGF-A, 0.2 μg	R158/184/270A, 15 μg	1.6	7
	R193/194A, 15 μg	3.0	5

chemotaxis of BCE cells, which was completely inhibited by endostatin at 100 ng/mL (Fig. 1*A*), as previously shown (31). The R193/194A mutant on the other hand failed to inhibit the FGF-2–induced chemotaxis. VEGF-A stimulated a slightly stronger chemotactic response of BCE cells compared with FGF-2, which was blocked in the presence of endostatin at 100 ng/mL (Fig. 1*B;* refs. 22 and 24). The R193/194A mutant exerted a slight suppression of VEGF-A–induced chemotaxis; however, the migratory response was still evident compared with the basal condition. These results indicate that the 193/194 heparin-binding site in endostatin is an important mediator of its inhibitory effect on endothelial cell chemotaxis.

Peptide Encompassing Amino Acid Residues 180–199 in Endostatin Mimics the Effect of Full-Length Endostatin on Chemotaxis. Because the 193/194 arginine residues in endostatin were essential for inhibition of FGF-2–induced CAM angiogenesis and chemotaxis of primary endothelial cells, we tested a synthetic, 20 amino acid residue peptide corresponding to residues 180–199 in endostatin (peptide 180–199/wt), for its effect on BCE cell chemotaxis. Cells were stimulated to migrate toward FGF-2 in the presence or absence of peptide 180–199/wt, at 10 or 100 ng/mL. The higher concentration of peptide was required to block FGF-2–induced chemotaxis of BCE cells (Fig. 1*C*). A second peptide in which the two arginine residues at positions 193/194 were replaced by alanine (peptide 180–199/mut), was unable to inhibit FGF-2–induced chemotaxis of BCE cells at 100 ng/mL (Fig. 1*D*). These results show that amino acids 180–199 in endostatin are sufficient for mediation of the inhibitory effect of endostatin on FGF-2–induced chemotaxis of primary endothelial cells and that the arginine residues in position 193/194 are required for this inhibition.

Effect of Peptide 180–199 on Fibrosarcoma Growth and Vascularization. On the basis of the critical role of arginines 193/194 in endostatin for its antiangiogenic effect, as judged by one *in vitro* and one semi-*in vivo* model, we decided to test the effect of peptide 180–199 on tumor growth and vascularization *in vivo*. C57BL6/J mice were inoculated subcutaneously with T241 fibrosarcoma cells on their left flank and when the tumors were palpable (~50 mm^3) after 4 to 6 days, a daily treatment was initiated with endostatin, peptide 180–199/wt and peptide 180–199/mut, all at 25 mg/kg/day. Although this represents a higher molar concentration of peptide, the same dose of endostatin and peptides was chosen for the tumor treatments. This decision was based on the fact that 100 ng/mL of peptide 180–199/wt was required to inhibit FGF-2–induced chemotaxis of endothelial cells (Fig. 1*C*), the same concentration as for endostatin. Human IgG was used as a control. The treatments were given as subcutaneous injections in the right flank for 11 days. No effect on tumor growth was seen during this period of treatment (Fig. 2*A*).

Tumor material was fixed and embedded in paraffin for sectioning. During this process the tumors were divided in two (Fig. 2*B*). This revealed that tumors from mice treated with peptide 180–199/wt were much whiter in appearance than tumors from mice treated with peptide 180–199/mut (Fig. 2*B*), possibly because of reduced vascularization. Immunohistochemical staining against CD31 on tumor sections from the four treatment groups indeed showed different patterns of vascularization (Fig. 2*C*). Tumors from control mice had large dilated vessels present throughout the tissue. This was in contrast to tumors from mice treated with endostatin or peptide 180–199/wt, which displayed fewer vessels of a smaller diameter. The vessels in tumors from mice treated with peptide 180–199/mut appeared significantly larger than those from mice treated with endostatin or peptide 180–199/wt (Fig. 2*C*).

We quantified vascular parameters as described previously (30) on three different tumors from each treatment group. This method of quantifying tumor angiogenesis relates the length, volume, and surface area of the vessels to tumor volume. The results show that all three vascular parameters determined in tumors from endostatin-treated mice were reduced (Fig. 2*D*). The effect on vessel volume was most striking, with a 90% reduction in tumors treated with full-length endostatin or the 180–199/wt peptide compared with control treatment. In contrast, vascularization of tumors from mice treated with peptide 180–199/mut was not changed significantly from the control.

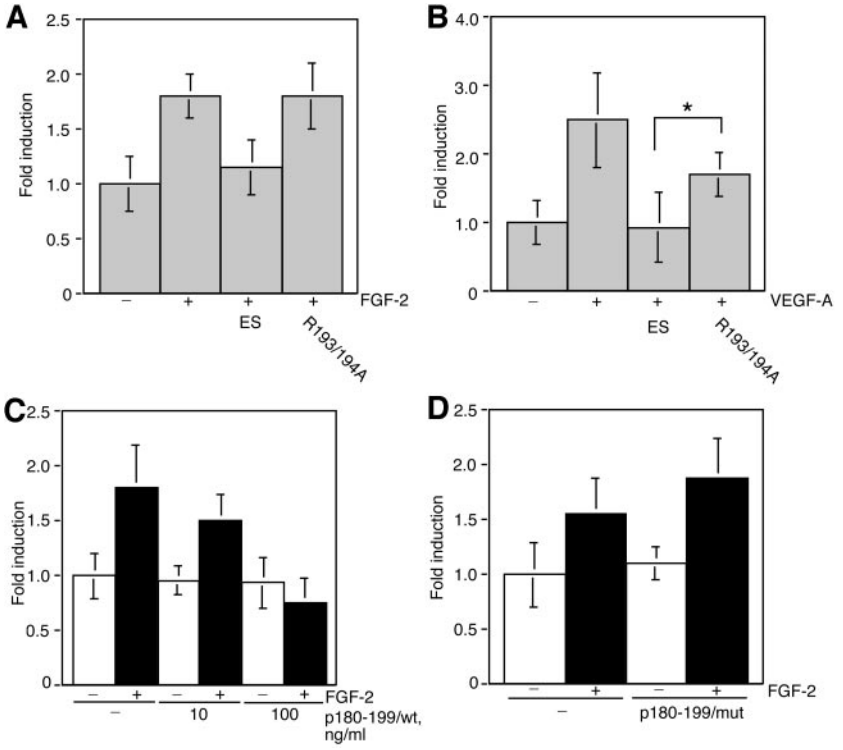

Fig. 1. Inhibition of growth factor-induced endothelial cell chemotaxis by endostatin is mediated by its minor heparin-binding site. *A*, chemotaxis of primary BCE cells induced by FGF-2 was inhibited in the presence of 100 ng/mL endostatin (ES). Inclusion of an endostatin mutant in which arginines 193/194 had been replaced by alanine residues (R193/194A) failed to inhibit FGF-2–induced chemotaxis. *B*, VEGF-A–induced chemotaxis of BCE cells was completely arrested by endostatin. The R193/194A mutant exerted a slight suppression of VEGF-A–induced chemotaxis, but the majority of the response remained. *C*, a synthetic peptide corresponding to amino acid residues 180–199 in endostatin (p180–199/wt) inhibited FGF-2–induced chemotaxis at a concentration of 100 ng/mL. *D*, substitution of the two arginines in position 193/194, in peptide 180–199/wt, to alanines (peptide 180–199/mut) resulted in loss of the inhibitory effect on FGF-2–induced chemotaxis. Peptide 180–199/mut was used at 100 ng/mL. *Error bar* indicates 1 SD. *, $P < 0.05$.

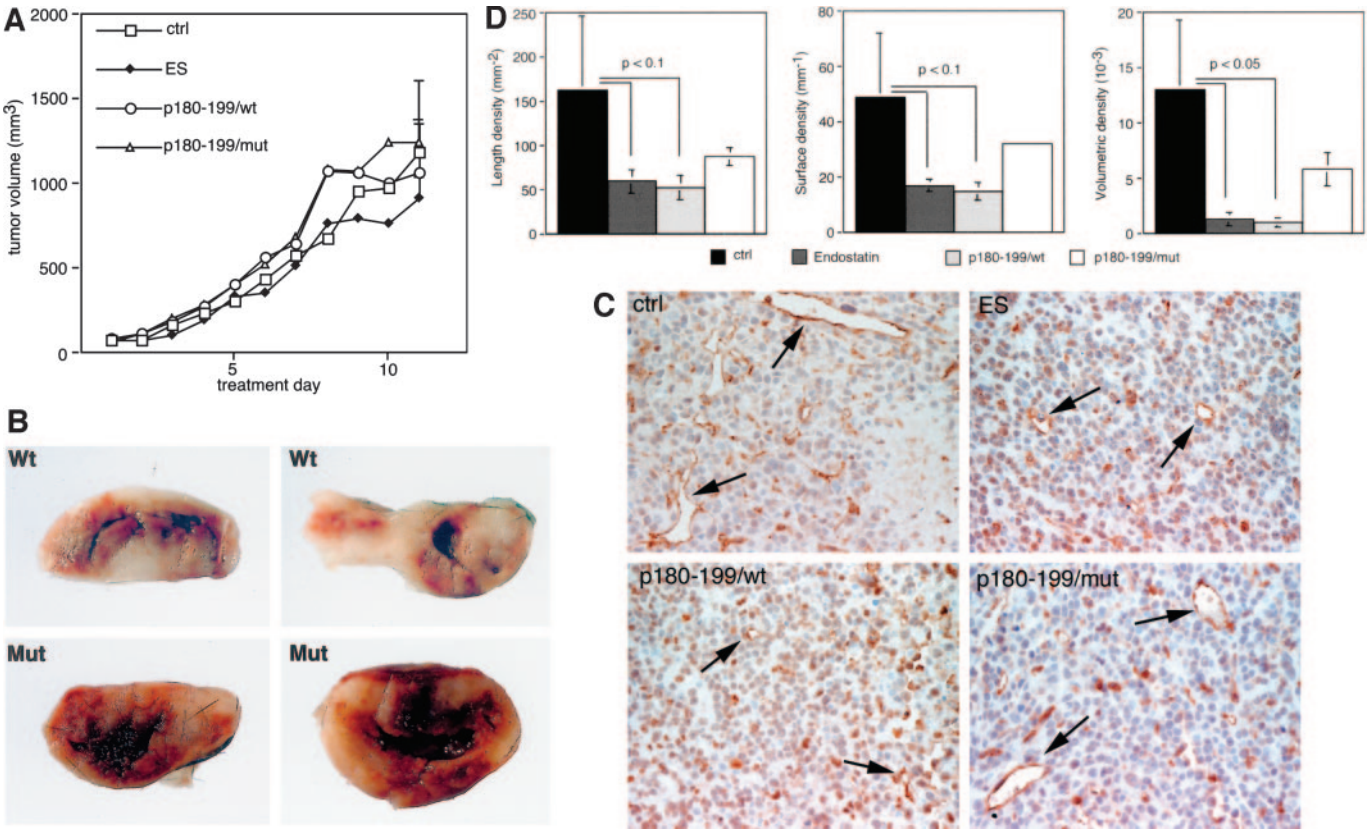

Fig. 2. A synthetic peptide corresponding to amino acids 180–199 of endostatin reduces vascularization of fibrosarcoma tumors. *A*, C57BL6/J mice bearing palpable (~50 mm^3) fibrosarcoma tumors were treated daily with subcutaneous injections of IgG (ctrl), endostatin (ES), peptide (p) 180–199/wt or peptide 180–199/mut for 11 days. Endostatin and peptides were administered at 25 mg/kg/day. Tumor volumes were measured daily with a caliper. *B*, tumors from mice treated with either peptide 180–199/wt (Wt; *top panels*) or peptide 180–199/mut (Mut; *bottom panels*). *C*, immunohistochemical staining for CD31 on paraffin sections of tumors from mice treated with IgG (ctrl), endostatin (ES), peptide (p) 180–199/wt, and peptide 180–199/mut. *Arrows* indicate some of the vessels. Photographed at ×40 magnification. *D*, stereological quantification of vascular parameters in tumors from mice treated with IgG (ctrl), endostatin, peptide 180–199/wt, and peptide 180–199/mut. *Error bar* indicates 1 SD. Statistically significant results are indicated by $P < 0.1/0.05$.

These results show that an endostatin-derived synthetic peptide covering amino acid 180–199 reduces tumor vascularization *in vivo*, an effect dependent on the minor heparin-binding site in endostatin.

Effect of Peptide 180–199 on Pancreatic Carcinoma Growth and Vascularization. Because peptide 180–199 had no effect on T241 fibrosarcoma growth but reduced tumor vascularization in the same model, we decided to further test the effect of peptide 180–199/wt and peptide 180–199/mut in a slow-growing tumor model, BxPC3 human pancreatic carcinoma. SCID mice were inoculated subcutaneously with BxPC3 pancreatic carcinoma cells on their left flank, and when the tumors had reached a size of approximately 100 mm^3 (after 2 weeks), treatment was initiated. Continuous delivery of endostatin with mini-osmotic pumps implanted intraperitoneally in mice has been shown to be more efficient and to require a lower dose to achieve the same antitumor effect, as compared with a single daily bolus administration of endostatin in this tumor model (32). We therefore used mini-osmotic pumps to administer the two peptides at 25 mg/kg/day for 3 weeks. Because peptide 180–199/mut did not have any significant effects either on chemotaxis (Fig. 1*D*) or on tumor vascularization (Fig. 2*D*), it was considered a control treatment. Mean tumor volumes from the two treatment groups are shown in Fig. 3*A*. Figure 3*B* shows individual tumor volumes from the two treatment groups. Treatment with peptide 180–199/wt resulted in a large spread in tumor volume from complete regression to efficient and rapid growth. In contrast, tumors from mice treated with peptide 180–199/mut displayed a rather homogenous size (Fig. 3*B*). Because of the large spread in tumor volume in the group treated with peptide 180–199/wt, there was no statistically significant difference in tumor volume between the groups. Four tumors from each treatment group with volumes close to the mean (see bar in Fig. 3*B*) are shown in Fig. 3*C*.

We did immunohistochemical staining for CD31 on tumor sections from three different tumors from each treatment group. Quantification of length, surface area, and volume of the tumor vessels (as described above) again revealed a decreased tumor vascularization in mice treated with peptide 180–199/wt compared with peptide 180–199/mut (Fig. 3*D*). On the basis of these results, we conclude that the arginine residues in positions 193 and 194 in endostatin are important for the antiangiogenic effect of endostatin.

DISCUSSION

There are two heparin-binding sites in endostatin; a major site encompassing arginine residues 155/158/184/270 and a minor including arginines 193/194 (15, 23). Our data show that inhibition of FGF-2–induced CAM angiogenesis by endostatin was dependent on both the major and the minor heparin-binding site, whereas inhibition of VEGF-A–induced CAM angiogenesis was dependent only on the minor heparin-binding site. These data in combination with our previous study (33) indicate that endostatin inhibits vessel formation stimulated by FGF and VEGF through overlapping but distinct mechanisms, probably reflecting differences in the endothelial cell surface protein expression in response to the two growth factors. The fact that the major heparin-binding site was critical for the mechanism of action of endostatin only in FGF-2–treated cells implies a high degree of specificity in the interaction between endostatin and heparin/

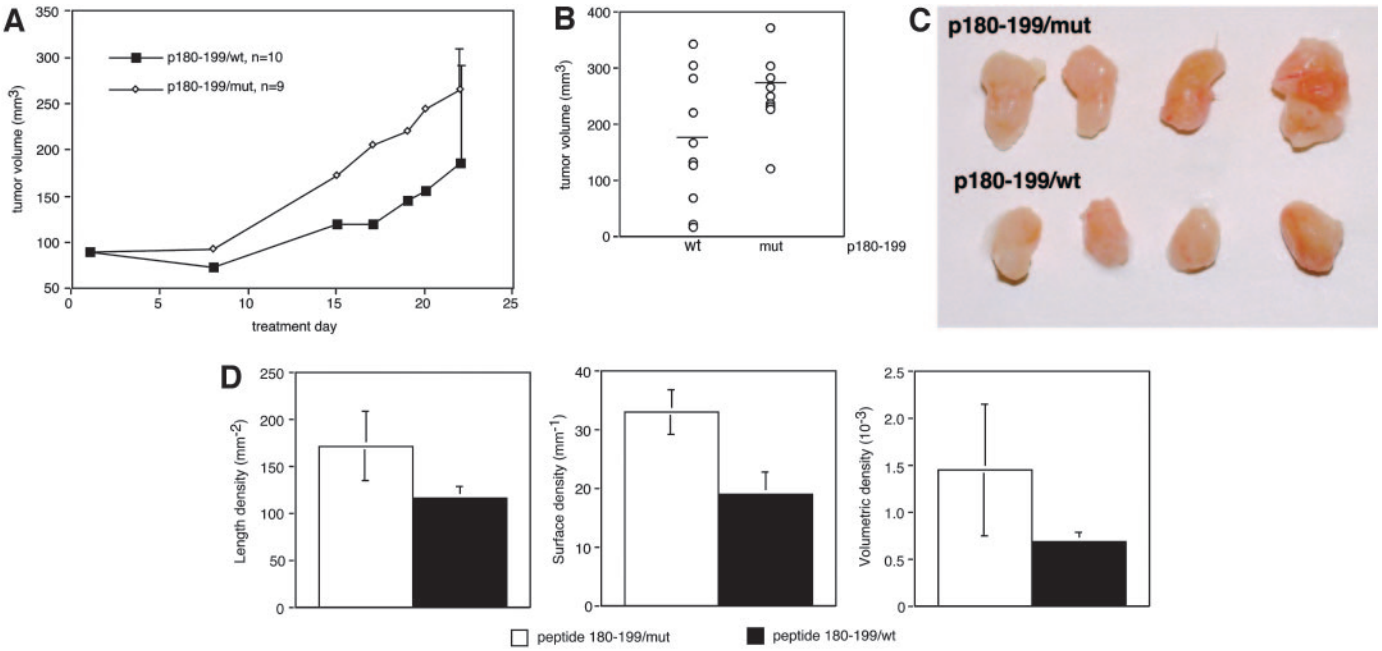

Fig. 3. Arginines 193/194 in the endostatin-derived peptide 180–199/wt mediate reduced vascularization of pancreatic carcinoma tumors. *A*, SCID mice with established pancreatic carcinoma tumors (~100 mm^3) were treated for 3 weeks with either peptide (p) 180–199/wt or peptide 180–199/mut. Peptides were administered at 25 mg/kg/day using mini-osmotic pumps implanted intraperitoneally. Tumor volumes were measured with a caliper. *B*, individual tumor volumes (indicated by a *circle*) in the two treatment groups, last day of the study. The *bar* indicates mean tumor volume of the group. *C*, four tumors from each treatment group with volumes close to the mean. *D*, stereological quantification of vascular parameters in tumors from mice treated with peptide 180–199/wt or peptide 180–199/mut. *Error bar* indicates 1 SD.

heparan sulfates on the endothelial cell surface. This is supported by the specific structure of the heparin/heparan sulfate domain implicated in endostatin binding (24).

Our data that heparin binding is important in the function of endostatin as an angiogenesis inhibitor agree with and extend our previous reports (21, 33) as well as those by Wickström *et al.* (19, 34). Wickström *et al.* have implicated the two major suggested cell surface targets of endostatin (integrin $\alpha5\beta1$ and heparan sulfate) in its antiangiogenic action, by showing that both integrin $\alpha5\beta1$ and heparan sulfate proteoglycan are required for localization of endostatin to lipid rafts. This localization is in turn critical for the downstream signaling events induced by endostatin, such as down-regulation of RhoA activity (19) and disassembly of the actin cytoskeleton (19, 21).

We investigated the antiangiogenic properties of a synthetic peptide of human endostatin, including arginines 193/194. This peptide (peptide 180–199/wt), but not a mutant R193/194A peptide (peptide 180–199/mut), inhibited FGF-2–induced chemotaxis of primary endothelial cells. Furthermore, *in vivo* vascularization of highly aggressive fibrosarcoma tumors was decreased by treatment with peptide 180–199/wt. In contrast, tumor vascularization in animals treated with the 180–199/mut peptide was not significantly different from that in tumors from control-treated animals. However, we cannot exclude that antiangiogenic effects, independent of the heparin binding, are mediated by this stretch in endostatin. That would be in agreement with the partial reduction in VEGF-A–induced chemotaxis by the full-length endostatin mutant R193/194A (Fig. 1*B*). Although tumor vascularization was substantially reduced after endostatin or peptide 180–199/wt treatment of mice bearing T241 fibrosarcoma, no effect was seen on tumor growth during the treatment period. Tumor vessels are known to be dysfunctional, and it is possible that a considerable part of the tumor vasculature is dispensable. Even so, it is surprising that the 90% decreases in vessel parameters induced by endostatin or the 180–199 wt peptide (see Fig. 2*D*) did not arrest growth of the tumors. For ethical reasons, the tumor study had to be interrupted; it is possible that a larger tumor burden would have been more dependent on the vessel supply.

Tumor vascularization differed also between mice with pancreatic carcinomas (BxPC3), treated with either peptide 180–199/wt or peptide 180–199/mut. Again, animals treated with the mutant R193/194A peptide displayed a significantly higher degree of tumor vascularization compared with mice treated with peptide 180–199/wt. Tumor volumes in the group treated with peptide 180–199/mut showed small deviations from the mean. However, in the group treated with peptide 180–199/wt, tumor volumes ranged from large to almost regression. Why some of the tumors responded to treatment with peptide 180–199/wt, whereas some did not, is unclear. Thus, although vascularization was reduced in both T241 and BxPC3 tumors after treatment with peptide 180–199/wt, a tendency for effect on tumor volume was observed only in the BxPC3 pancreatic carcinoma model. Endostatin is known to be a less potent inhibitor of tumor growth in fast-growing experimental models such as T241 (32). Furthermore, in the BxPC3 study, intraperitoneal mini-osmotic pumps were used for an even delivery of endostatin. This strategy has been shown to yield a more efficient treatment and to require a lower dose to achieve the same antitumor effect than a single daily bolus administration of endostatin (32).

There are other recently published studies reporting antiangiogenic effects of endostatin-derived peptides (34–37). Interestingly, the 11 amino acid long peptide (ES-2) used by Wickström *et al.* has a nine residue overlap with peptide 180–199 used by us, and includes R193/194. ES-2 was shown to bind to endothelial cells via $\beta1$- and heparin-dependent mechanisms, inducing cytoskeletal rearrangements and inhibition of FGF–2-induced chemotaxis at concentrations in the milligram range. These effects were dependent on the heparin-binding R193/194 in the peptide (34). The motif required for integrin-binding of the ES-2 peptide was not identified. Endostatin-derived peptides of approximately 40 to 50 amino acids, covering nearly the entire sequence of endostatin, have been tested for antiangiogenic activity

(37). Two studies that used identical endostatin-derived fragments (35, 36) show that the most NH_2-terminal and COOH-terminal fragments of endostatin confer antiangiogenic activity. A third study using similar peptides show antiangiogenic activity only of the COOH-terminal fragment (37). None of the peptides that were reported to be antiangiogenic covered the minor heparin-binding site. The reason for the discrepancy between these results on one hand, and those reported in this study and by Wickström *et al.* on the other, is not clear. However, the significantly longer peptides used, compared with peptide 180–199 (20 amino acids) and ES-2 (11 amino acids), could affect folding and the secondary structure of the peptides. Both from a mechanistic and clinical perspective, it would be interesting to find the shortest possible endostatin-derived peptide that still retains the antiangiogenic and antitumorigenic activity.

REFERENCES

1. Risau W. Mechanisms of angiogenesis. Nature (Lond) 1997;386:671–4.
2. Folkman J. Angiogenesis in cancer, vascular, rheumatoid and other disease. Nat Med 1995;1:27–31.
3. Folkman, J. Tumor angiogenesis. In: Holland JF, Frei EI, Bast RCJ, Kufe DW, Pollock RE, Weichselbaum RR, editors. Cancer Medicine, 5th edition, Ontario, Canada: B. C. Decker Inc; 2000. p. 132–52.
4. Hanahan D, Weinberg RA. The hallmarks of cancer. Cell 2000;100:57–70.
5. Carmeliet P, Jain RK. Angiogenesis in cancer and other diseases. Nature (Lond) 2000;407:249–257.
6. Cross MJ, Claesson-Welsh L. FGF and VEGF function in angiogenesis: signalling pathways, biological responses and therapeutic inhibition. Trends Pharmacol Sci 2001;22:201–7.
7. Javerzat S, Auguste P, Bikfalvi A. The role of fibroblast growth factors in vascular development. Trends Mol Med 2002;8:483–9.
8. Ferrara N, Gerber HP, LeCouter J. The biology of VEGF and its receptors. Nat Med 2003;9:669–76.
9. O'Reilly MS, Boehm T, Shing Y, et al. Endostatin: an endogenous inhibitor of angiogenesis and tumor growth. Cell 1997;88:277–85.
10. Dixelius J, Cross MJ, Matsumoto T, Claesson-Welsh L. Endostatin action and intracellular signaling: beta-catenin as a potential target? Cancer Lett 2003;196:1–12.
11. Ma L, Elliott SN, Cirino G, Buret A, Ignarro LJ, Wallace JL. Platelets modulate gastric ulcer healing: role of endostatin and vascular endothelial growth factor release. Proc Natl Acad Sci USA 2001;98:6470–5.
12. Miosge N, Sasaki T, Timpl R. Angiogenesis inhibitor endostatin is a distinct component of elastic fibers in vessel walls. FASEB J 1999;13:1743–50.
13. Sasaki T, Fukai N, Mann K, Gohring W, Olsen BR, Timpl R. Structure, function and tissue forms of the C-terminal globular domain of collagen XVIII containing the angiogenesis inhibitor endostatin. EMBO J 1998;17:4249–56.
14. Yu Y, Moulton KS, Khan MK, et al. E-selectin is required for the antiangiogenic activity of endostatin. Proc Natl Acad Sci USA 2004;101:8005–10.
15. Sasaki T, Larsson H, Kreuger J, et al. Structural basis and potential role of heparin/heparan sulfate binding to the angiogenesis inhibitor endostatin. EMBO J 1999;18:6240–8.
16. Karumanchi SA, Jha V, Ramchandran R, et al. Cell surface glypicans are low- affinity endostatin receptors. Mol Cell 2001;7:811–22.
17. Rehn M, Veikkola T, Kukk-Valdre E, et al. Interaction of endostatin with integrins implicated in angiogenesis. Proc Natl Acad Sci USA 2001;98:1024–9.
18. Wickström SA, Alitalo K, Keski-Oja J. Endostatin associates with integrin alpha5beta1 and caveolin-1, and activates Src via a tyrosyl phosphatase-dependent pathway in human endothelial cells. Cancer Res 2002;62:5580–9.
19. Wickström SA, Alitalo K, Keski-Oja J. Endostatin associates with lipid rafts and induces reorganization of the actin cytoskeleton via down-regulation of RhoA activity. J Biol Chem 2003;278:37895–901.
20. Sudhakar A, Sugimoto H, Yang C, Lively J, Zeisberg M, Kalluri R. Human tumstatin and human endostatin exhibit distinct antiangiogenic activities mediated by alpha v beta 3 and alpha 5 beta 1 integrins. Proc Natl Acad Sci USA 2003;100:4766–71.
21. Dixelius J, Larsson H, Sasaki T, et al. Endostatin-induced tyrosine kinase signaling through the Shb adaptor protein regulates endothelial cell apoptosis. Blood 2000;95:3403–11.
22. Yamaguchi N, Anand-Apte B, Lee M, et al. Endostatin inhibits VEGF-induced endothelial cell migration and tumor growth independently of zinc binding. EMBO J 1999;18:4414–23.
23. Hohenester E, Sasaki T, Olsen BR, Timpl R. Crystal structure of the angiogenesis inhibitor endostatin at 1.5 A resolution. EMBO J 1998;17:1656–64.
24. Kreuger J, Matsumoto T, Vanwildemeersch M, et al. Role of heparan sulfate domain organization in endostatin inhibition of endothelial cell function. EMBO J 2002;21:6303–11.
25. Vallejo AN, Pogulis RJ, Pease LR. In vitro synthesis of novel genes: mutagenesis and recombination by PCR. PCR Methods Appl 1994;4:S123–130.
26. Poschl E, Mayer U, Stetefeld J, et al. Site-directed mutagenesis and structural interpretation of the nidogen binding site of the laminin gamma1 chain. EMBO J 1996;15:5154–9.
27. Friedlander M, Brooks PC, Shaffer RW, Kincaid CM, Varner JA, Cheresh DA. Definition of two angiogenic pathways by distinct alpha v integrins. Science (Lond) 1995;270:1500–2.
28. Auerbach R, Auerbach W, Polakowski I. Assays for angiogenesis: a review. Pharmacol Ther 1991;51:1–11.
29. Workman P, Balmain A, Hickman JA, et al. UKCCCR guidelines for the welfare of animals in experimental neoplasia. Lab Anim 1988;22:195–201.
30. Gundersen HJ, Bendtsen TF, Korbo L, et al. Some new, simple and efficient stereological methods and their use in pathological research and diagnosis. Apmis 1988;96:379–94.
31. Olsson AK, Larsson H, Dixelius J, et al. A fragment of histidine-rich glycoprotein is a potent inhibitor of tumor vascularization. Cancer Res 2004;64:599–605.
32. Kisker O, Becker CM, Prox D, et al. Continuous administration of endostatin by intraperitoneally implanted osmotic pump improves the efficacy and potency of therapy in a mouse xenograft tumor model. Cancer Res 2001;61:7669–74.
33. Sasaki T, Larsson H, Tisi D, et al. Endostatins derived from collagens XV and XVIII differ in structural and binding properties, tissue distribution and anti-angiogenic activity. J Mol Biol 2000;301:1179–90.
34. Wickström SA, Alitalo K, Keski-Oja J. An endostatin-derived peptide interacts with integrins and regulates actin cytoskeleton and migration of endothelial cells. J Biol Chem 2004;279:20178–85.
35. Cattaneo MG, Pola S, Francescato P, Chillemi F, Vicentini LM. Human endostatin-derived synthetic peptides possess potent antiangiogenic properties in vitro and in vivo. Exp Cell Res 2003;283:230–6.
36. Chillemi F, Francescato P, Ragg E, Cattaneo MG, Pola S, Vicentini L. Studies on the structure-activity relationship of endostatin: synthesis of human endostatin peptides exhibiting potent antiangiogenic activities. J Med Chem 2003;46:4165–72.
37. Morbidelli L, Donnini S, Chillemi F, Giachetti A, Ziche M. Angiosuppressive and angiostimulatory effects exerted by synthetic partial sequences of endostatin. Clin Cancer Res 2003;9:5358–69.